Nano Research 2016, 9(6): 1775–1784
DOI 10.1007/s12274-016-1070-5
Research Article
ISSN 1998-0124
CN 11-5974/O4

A novel oscillator based on heterogeneous carbon@MoS_2 nanotubes

Wugui Jiang[1] (✉), Yonghui Zeng[1], Qinghua Qin[2] (✉), and Qianghui Luo[1]

[1] *School of Aeronautical Manufacturing Engineering, Nanchang Hangkong University, Nanchang 330063, China*
[2] *Research School of Engineering, the Australian National University, Acton ACT 2601, Australia*

Received: 7 January 2016
Revised: 27 February 2016
Accepted: 14 March 2016

© Tsinghua University Press and Springer-Verlag Berlin Heidelberg 2016

KEYWORDS
MoS_2 nanotubes,
carbon nanotubes,
oscillators,
hetero-nanotubes,
molecular dynamics

ABSTRACT

Oscillatory behavior of novel heterogeneous oscillators composed of carbon and molybdenum disulfide nanotubes (CNT@MST) was investigated for the first time, by using the methods of classical molecular dynamics. In the proposed oscillators, a molybdenum disulfide nanotube (MST) was set as an outer tube, leading to better compatibility with the semiconductor industry standards. A smooth and stable oscillator with a frequency reaching 20 GHz was obtained based on a double-walled CNT@MST hetero-nanotube for a wide range of gap widths, indicating that the proposed oscillators perform much better than those built from double-walled carbon nanotubes (CNTs) that require a narrow range of gap widths. In addition, the oscillation characteristics of CNT@MST oscillators containing different inner and outer tube chirality were significantly better than those of CNT@MST oscillators containing two tubes with the same chirality.

1 Introduction

Carbon nanotubes (CNTs) [1], as a special form of nanoscale materials, have triggered a tremendous amount of experimental and theoretical investigations in the material science community [2–4]. The unique properties of CNTs make them promising for many applications in nanoelectromechanical systems (NEMS) [5, 6]. Similar to CNTs, several transition-metal chalcogenides, such as molybdenum disulphide (MoS_2) and wolfram disulphide (WS_2), were also suggested to form tubular structures as a consequence of their two-dimensional molecular nature [7, 8]. Previously, it was reported that most MoS_2 nanostructures are unique semiconductor materials [9–11], which is compatible with the current standards of semiconductor industry. It has also been suggested that MoS_2 nanostructures can be utilized in a wide spectrum of applications, such as solid lubricants [12], field-effect transistors (FET) [13], biosensors [14], and nonvolatile memory devices [15]. Because CNTs and MoS_2 nanotubes (MSTs) have analogous tubular structures, CNTs might promote the formation of tubular MoS_2 on the surface of CNTs in a hydrothermal reaction

Address correspondence to Wugui Jiang, jiangwugui@nchu.edu.cn; Qinghua Qin, qinghua.qin@anu.edu.au

[16]. Song et al. [17] synthesized MoS_2-coated CNTs by using CNTs as a template and employing the hydrothermal synthesis method, and revealed that the inter-tube spacing between the fabricated CNTs and MSTs is ~0.44 nm in all studied coated structures. Zhang et al. [18] suggested that nanocomposites of CNT@MST could provide extremely low coefficients of friction and wear rates under rigorous wear testing at room and elevated temperatures. Currently, hetero-nanostructures of CNT@MST composites are promising highly composite functional materials, with potentially novel properties and applications [19, 20], owing to the combination of the unique physical, chemical, and mechanical properties of carbon and MoS_2 nanotubes.

It should also be mentioned that intensive studies have been conducted on one-dimensional MoS_2 and WS_2 nanotubes owing to their exceptional physical and chemical properties [21, 22]. Maharaj and Bhushan [23] conducted nanoindentation and compression tests to determine nanomechanical behavior of MoS_2 and WS_2 nanotubes. Lorenz et al. [24] used the density functional-based tight binding method to formulate the MoS_2 nanotube Young's modulus and Poisson's ratio as functions of the tube diameter and chirality. Kis et al. [25] measured shear and Young's moduli of MoS_2 nanotube ropes by using atomic force microscopy (AFM). Li et al. [26] studied mechanical properties and strain effects on the electronic structure of MoS_2 nanotubes by using the density functional theory. Xiao et al. [27] theoretically investigated the electronic structure and carrier mobility of armchair and zigzag MoS_2 nanotubes, again by using the density functional theory.

By contrast, very few papers reported molecular dynamics (MD) simulations of MoS_2 nanotube systems. Using the MD modeling approach, Enyashin and Ivanovskii [28, 29] performed MD simulations of capillary imbibition of molten KI into a MoS_2 nanotube and capillary filling of MoS_2 nanotubes. Bucholz and Sinnott [30] investigated the mechanical behavior of different types of MoS_2 nanotubes subjected to external compressive, tensile, and torsional loading.

In this paper, we present a novel nanoscale oscillator that combines the unique physical, chemical, and mechanical properties of both CNTs and MSTs. In the proposed oscillator, an MST was set as an outer tube owing to its unique semiconductor property, and a CNT was set as a core tube, because its atomic mass is smaller than that of the MST. The oscillation characteristics of the obtained CNT@MST hetero-nanotubes were investigated by employing the classical MD method. In particular, we thoroughly investigated the effect of the gap between the two tubes and the effect of the tube chirality on the oscillation amplitude and frequency, and on the stability of the inner tube.

2 Methodology

In our MD simulations, we employed the second generation reactive empirical bond-order (REBO) potential [31] to account for the intratubal atomic interaction of the CNT. On the other hand, the atomic interaction of the MST was calculated by using the Stillinger–Weber (SW) potential [32], which has been successfully used to predict the mechanical properties of MoS_2 by Jiang et al. [33–35]. Two potentials mediate interactions between non-bonded atoms, the van der Waals potential and the electrostatic potential. In most previous studies of interactions in multiwalled carbon nanotubes [3, 36, 37] and MoS_2/graphene hetero-structures [38], only the Lennard–Jones (LJ) 12-6 potential was considered because the electrostatic interaction is very weak compared with the van der Waals interaction. Thus, in the present study the interaction between the MST and the CNT was modeled by using the LJ 12-6 potential. The LJ interaction can be written as $U_{LJ}(r_{ij}) = 4\varepsilon[(\sigma/r_{ij})^{12} - (\sigma/r_{ij})^{6}]$ ($r_{ij} \leqslant r_C$), where r_{ij} is the distance between the atoms (that do not form a bond), ε is the well depth, σ is the size parameter, and r_C is the cutoff distance. The Lorentz–Berthelot (LB) mixing rule [39–41] was used to determine the well-depth and size parameters, i.e., the ε and σ of the Mo–C and S–C interactions, as listed in Table 1. In order to verify the applicability of the LB mixing rule for determining the ε and σ parameters, the LJ interaction of the C–C was calculated first, and the calculation results agreed well with the results obtained by using the adaptive intermolecular reactive empirical bond order (AIREBO) potential [42], also shown in Table 1. The cutoff distance r_C should be set to 2.2σ or larger, according to the statement in Refs. [43–45]; consequently, in our simulations the

cutoff distance was set to 10 Å. These potential parameters were used to estimate the binding energy of CNT@MST hetero-nanotubes with different inter-tube gap widths. Figure 1 shows the simulated binding energy vs. the inter-tube gap width between the CNT and MST. The potential energy minimum is observed for the inter-tube gap width of 0.367 nm, with the corresponding binding energy of –19.21 meV. These two values are close to the values obtained from the first-principles calculations, 0.366 nm and –21.0 meV, respectively [46].

Table 1 Lennard–Jones parameters for the interatomic van der Waals interactions

	Mo–C	S–C	C–C^{LB}	C–C^{AIREBO}
σ (Å)	3.076	3.514	3.432	3.400
ε (eV)	0.0033	0.0074	0.0045	0.0029

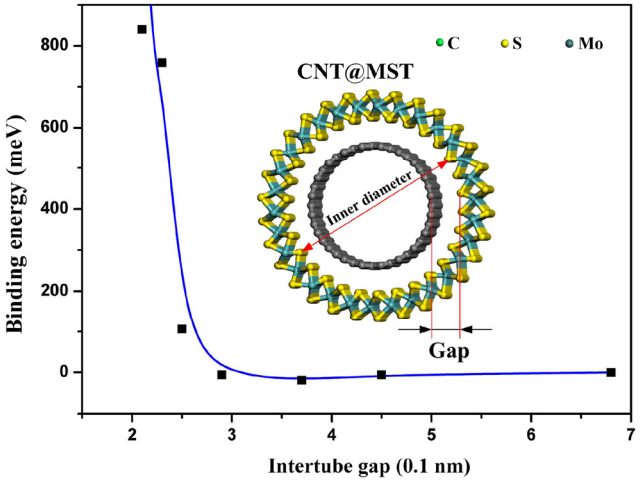

Figure 1 Binding energy (per carbon atom) as a function of the inter-tube gap width between CNT and MST. Inset shows the view of CNT@MST hetero-nanotubes. The solid line represents the fitting curve.

The internal configuration of a CNT is characterized by a pair of its chiral indices (n, m). Similar to the description of the CNT chirality, different types of MSTs are distinguished based on the specific lattice vector for the nanotube wrapping, which may be described in terms of the primitive two-dimensional (2D) lattice vectors $\vec{a_1}$ and $\vec{a_2}$ and two integer indices: $\vec{c} = n\vec{a_1} + m\vec{a_2}$, where $\vec{c}$ is the curl vector and n, m are integers. Based on the (n, m) indices of a given nanotube, three classes of MSTs can be distinguished: $n = m$ "armchair" nanotubes, $n \neq 0$, $m = 0$ "zigzag" nanotubes, and $n \neq m$ "chiral" nanotubes. For both CNTs and MSTs, only armchair and zigzag nanotubes were considered in the present work. In all of the heterogeneous modes, the outer tube was an MST while the inner tube was a CNT. To study the effect of the inter-tube gap width and tube chirality on the dynamics, 4 MSTs with (14, 14), (15, 15), (24, 0), and (26, 0), and 7 CNTs with (12, 0), (16, 0), (18, 0), (20, 0), (22, 0), (24, 0), and (9, 9) were employed. The respective nine oscillator modes were: CNT(12, 0)@MST(15, 15), CNT(16, 0)@MST(15, 15), CNT(18, 0)@MST(15, 15), CNT(20, 0)@MST(15, 15), CNT(22, 0)@MST(15, 15), CNT(24, 0)@MST(15, 15), CNT(9, 9)@MST(14, 14), CNT(18, 0)@MST(26, 0), and CNT(9, 9)@MST(24, 0). Both the outer and inner tubes had open ends, and the outer tube was fixed in the simulations. More detailed geometric parameters of these oscillator modes are listed in Table 2.

Table 2 Geometric parameters and frequencies of oscillators based on CNT@MST, where the inner diameter is defined as shown in the inset of Fig. 1

CNT @MST	Length (Å)	Inner diameter (Å)	Gap (Å)	Atoms in tube	Frequency (GHz)
(12, 0)@(15, 15)	59.11/79.58	23.01/9.40	6.81	1,710/912	17.54
(16, 0)@(15, 15)	59.11/79.56	23.01/12.53	5.24	1,710/1,216	18.52
(18, 0)@(15, 15)	59.11/79.57	23.01/14.10	4.46	1,710/1,368	19.61
(20, 0)@(15, 15)	59.11/79.57	23.01/15.67	3.67	1,710/1,520	23.26
(22, 0)@(15, 15)	59.11/79.57	23.01/17.23	2.89	1,710/1,672	20.83
(24, 0)@(15, 15)	59.11/79.57	23.01/18.80	2.11	1,710/1,824	Unstable
(9, 9)@(14, 14)	59.08 /79.97	23.01/12.21	4.47	1,596/1,170	19.92
(18, 0)@(26, 0)	59.23/79.57	23.01/14.01	4.44	1,716/1,368	19.80
(9, 9)@(24, 0)	59.21/79.97	23.01/12.21	4.38	1,584/1,170	21.28

Initially, the two tubes in each mode had symmetrical layouts along the axes, and the tubes were concentric. The system of the two tubes was put in a heat bath at the temperature of ~100 K for 20 ps after energy minimization, and the total number of particles, the system's volume, and the absolute temperature were constant (corresponding to the canonical NVT ensemble, where N is the total number of particles in the system, V is the system's volume, and T is the absolute temperature). Then, the axial velocity constraint of 0.1 nm/ps was applied to the inner tube for 30 ps under constant temperature. After 30 ps, the velocity constraint on the inner tube was removed, and the tube began to oscillate in the axial direction under the condition of constant energy, for 2,500 ps (corresponding to the microcanonical NVE ensemble, where NV is the same as above and E is the total energy in the system). In all simulations, the time step was 1 fs.

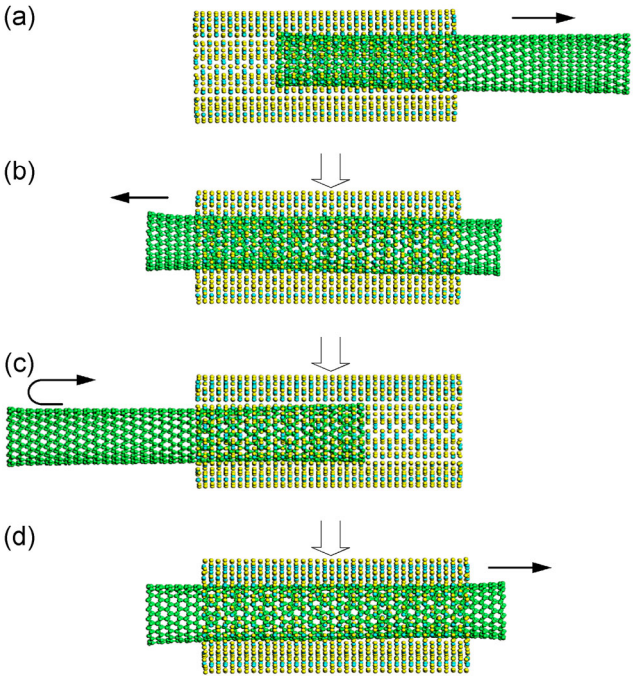

Figure 2 Snapshots of the periodical oscillation of the CNT(18, 0)@MST(15, 15) oscillator.

3 Results and discussion

3.1 *Gap effect*

Figures 2(a)–2(d) show a periodic oscillation for the CNT(18, 0)@MST(15, 15) oscillator. The extruded inner tube as shown in Fig. 2(a) retracts back into the outer tube (Fig. 2(b)) along the axial direction, owing to the restoring force generated by the van der Waals interaction acting on the extruded tube. As a consequence, the kinetic energy of the inner tube gradually decreases. When the kinetic energy of the inner tube reaches zero (that is, when the potential energy reaches its maximum) the tube has moved to its leftmost position and the inner tube inverts (Fig. 2(c)). The kinetic energy reaches its maximum when the inner tube again completely merges with the outer tube (Fig. 2(d)); meanwhile, the potential energy reaches its minimum. This completes one cycle of the periodic oscillatory motion of the inner tube.

We define the inter-tube gap width as the distance between the S atoms in the MST and the C atoms in the CNT, as shown in the inset of Fig. 1. The position of the mass center of the inner tube (MCIT), the velocity, and the overall van der Waals force along the axial direction of the inner tube are plotted in Figs. 3–5, respectively, for different inter-tube gap widths. It should be noted that the gap widths between the outer tube and the inner tube of CNT(12, 0)@MST(15, 15), CNT(16, 0)@MST(15, 15), CNT(18, 0)@MST(15, 15), CNT(20, 0)@MST(15, 15), CNT(22, 0)@MST(15, 15), and CNT(24, 0)@MST(15, 15) are 0.681, 0.524, 0.446, 0.367, 0.289, and 0.211 nm, respectively. For the above modes, except for CNT(24, 0)@MST(15, 15), the oscillations are stable, although the oscillation amplitudes decrease gradually with time but at different rates, as shown in Fig. 3. The oscillation is unstable with respect to time for the CNT(24, 0)@MST(15, 15) hetero-nanotube system, which corresponds to the minimal inter-tube gap considered in our simulations. It can be seen that the decay of the oscillation amplitude becomes weaker as the gap width between the two tubes decreases from 0.681 to 0.367 nm; however, for gap widths below 0.367 nm the oscillation amplitude decays faster. The reduction in the inner tube axial velocity can be clearly observed in Fig. 4, which is in accordance with the variation of the oscillation amplitude. By examining the overall van der Waals force on the inner tube in the axial direction (Fig. 5), we found that the interaction between the two tubes becomes progressively stronger as the gap width decreases. This implies that a narrower gap yields a stronger interaction for the inner tube,

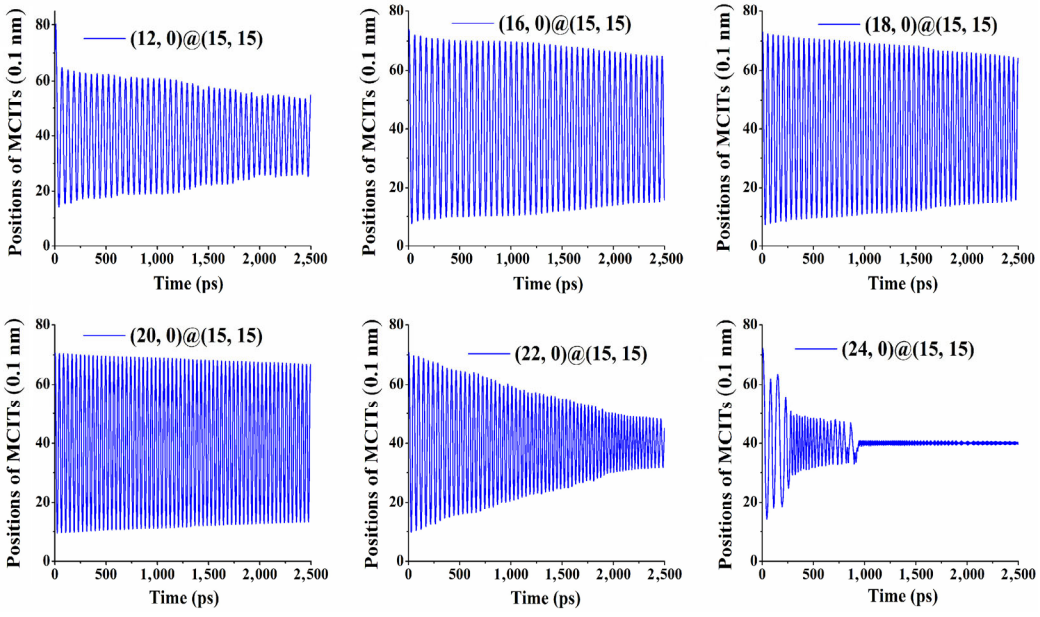

Figure 3 Histories of MCITs vs. time, for investigating the gap width effect.

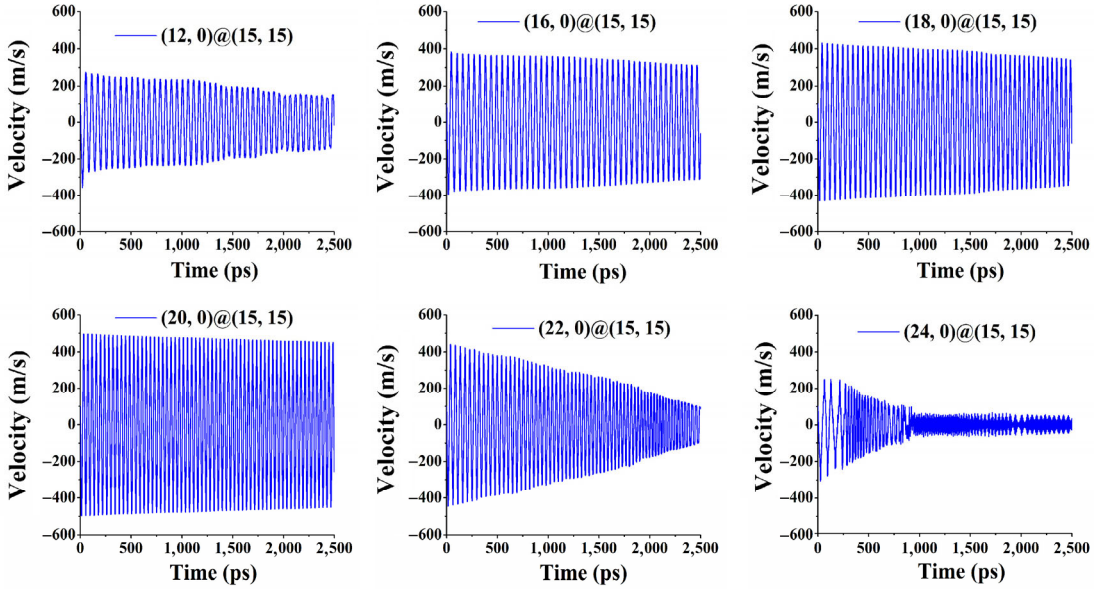

Figure 4 Oscillation velocities in the axial direction of the inner tubes, vs. time.

which in turn yields a higher resultant force (Fig. 5), thus leading to a higher velocity for the inner tube to tunnel through the outer tube (Fig. 4). However, if the gap width is further reduced toward a critical value, the increasing friction between the two tubes starts to significantly impede the oscillation of the inner tube. This results in an unstable restoring force of the van der Waals interaction, which is similar to what has been obtained in some previous studies [47–49] regarding the oscillation characteristics of double-walled carbon nanotube (DWCNT) oscillators.

As mentioned above, a wider gap implies a weaker friction effect on the oscillation of the inner tube, but it gives rise to a more significant off-axial rocking motion of the inner tube. Figure 6 shows the profile of the off-axial rocking motion of the inner tube for the CNT(12, 0)@MST(15, 15) system. The off-axial rocking motion profiles for the six oscillators are shown in Fig. 7 vs. time, and it is seen that the rocking motion of the inner tube becomes more significant with

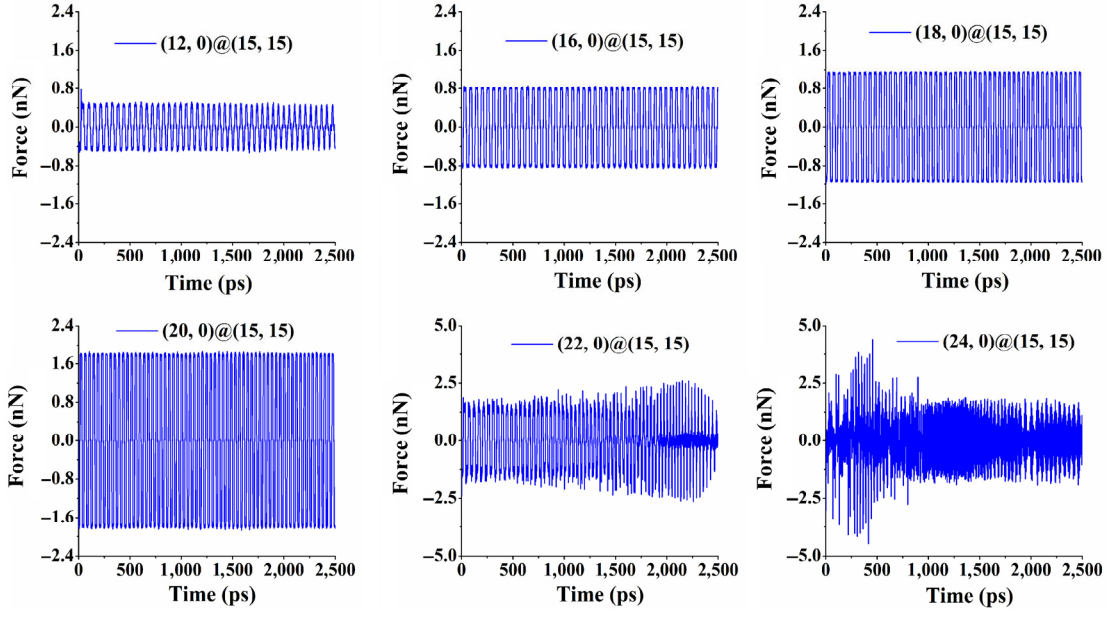

Figure 5 The resultant van der Waals forces in the axial direction of the inner tubes, vs. time.

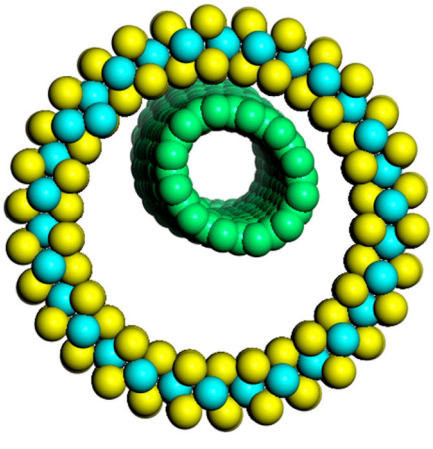

Figure 6 Cross-sections of the off-axial rocking motion of the inner tube, for the CNT(12, 0)@MST(15, 15) oscillator.

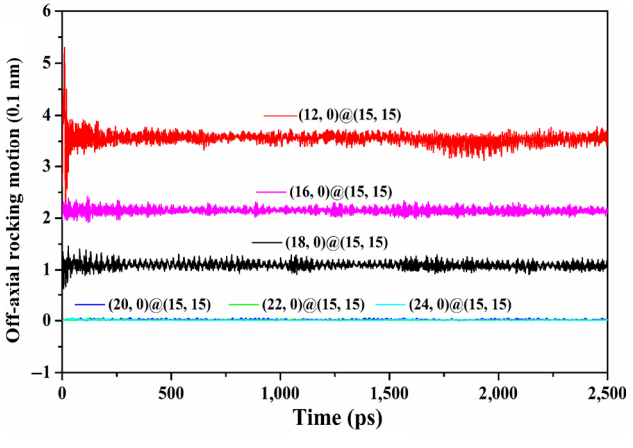

Figure 7 Off-axial rocking motions of inner tubes, vs. time, for investigating the gap width effect.

increasing the inter-tube gap width. The rocking motion of the inner tube may make the inner tube collide with the outer tube during the oscillation, resulting in the dissipation of the energy of the inner tube and consequently leading to the decay of the oscillation amplitude of the inner tube. Zhao et al. [50] also reported that the rocking motion of the inner tube yields poor oscillations, based on DWCNTs. In other words, a narrower gap implies a stronger off-axial rocking motion but a larger friction effect; that is, the off-axial rocking motion and the friction oppositely depend on the gap width parameter.

3.2 *Chirality effect*

Considering the fabrication of CNT@MST hetero-nanotubes and the above-mentioned inter-tube gap width effect [17], four double-walled hetero-nanotubes—CNT(9, 9)@MST(14, 14), CNT(18, 0)@MST(26, 0), CNT(9, 9)@MST(24, 0), and CNT(18, 0)@MST(15, 15)—were chosen for investigating the influence of chirality on the oscillation characteristics. In these studies, the gap width between the inner tube and the outer tube was ~0.44 nm. The detailed geometrical parameters are listed in Table 2. Figure 8 shows the variation in the

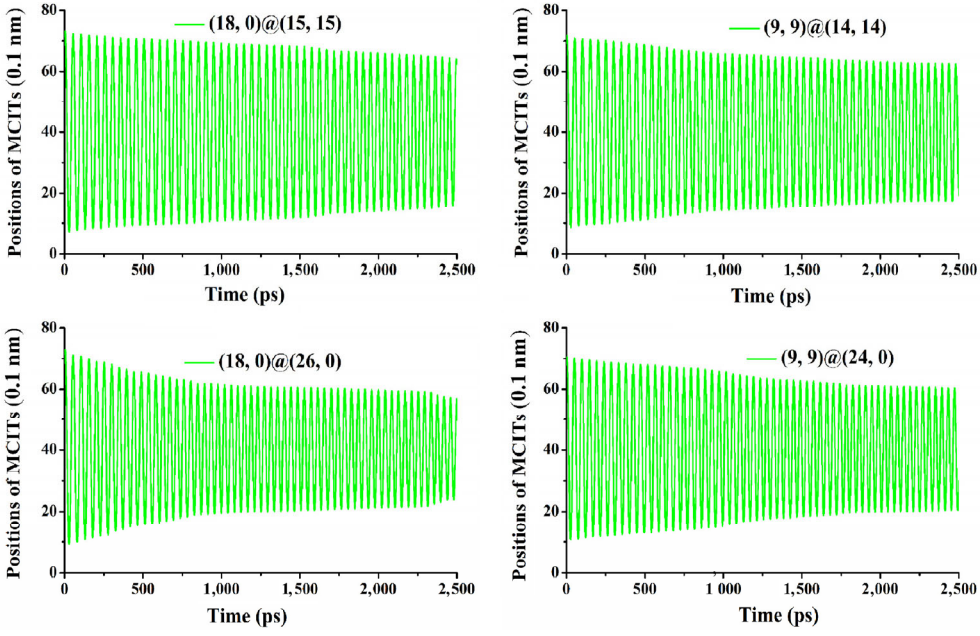

Figure 8 The MCITs of the inner tubes, vs. time, for investigating the chirality effect.

MCIT positions for the four hetero-nanotubes. It can be clearly seen from Fig. 8 that the dissipation rates of the oscillation amplitude for the CNT(18, 0)@MST(15, 15) and CNT(9, 9)@MST(24, 0) systems are smaller than those for the CNT(9, 9)@MST(14, 14) and CNT(18, 0)@MST(26, 0) systems. In other words, the oscillation amplitudes of the inner tubes in the hetero-nanotubes with different inner and outer tube chirality decay faster than those for the systems with the same inner and outer tube chirality, which is similar to the oscillation characteristics of double-walled CNTs which demonstrate that incommensurate double-wall CNTs exhibit much smoother oscillations compared with the commensurate ones [51, 52]. Figure 9 shows the off-axial rocking motion of these four oscillators, spanning the range from 0.08 to 0.14 nm. In addition, the off-axial rocking motion of CNT(18, 0)@MST(15, 15) and CNT(9, 9)@MST(24, 0) oscillators (with different inner and outer tube chirality) is obviously weaker than that of CNT(9, 9)@MST(14, 14) and CNT(18, 0)@MST(26, 0) oscillators (with the same inner and outer tube chirality).

The oscillation frequencies of CNT–CNT oscillators decrease monotonically with increasing the inter-tube gap width, and stable and sustained oscillations are observed only for the inter-tube gap width of ~0.34 nm

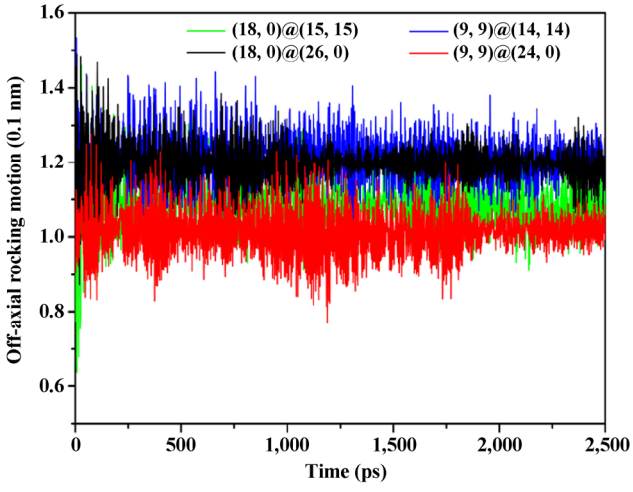

Figure 9 Off-axial rocking motions of inner tubes, vs. time, for investigating the chirality effect.

[37, 53, 54]. Qin et al. [3] suggested that the oscillation frequency of the inner tube should sensitively depend on the water structure in the gap. Table 2 lists the frequencies of all CNT@MST hetero-nanotubes that were studied in our simulations. We note that except the unstable (24, 0)@(15, 15) hetero-nanotube, the frequencies of the remaining oscillators in our simulations can reach gigahertz, and they increase as the gap width decreases down to 0.367 nm, and decrease as the gap decreases further (below 0.367 nm).

We found that a smooth and stable oscillator can be obtained based on CNT@MST hetero-nanotubes, in a wide range of gap width values, from 0.367 to 0.524 nm, demonstrating a stronger advantage over oscillators that are built from DWCNTs, which exhibit stable and sustained oscillations only when the inter-tube gap width is ~0.34 nm.

4 Conclusions

In summary, we proposed a conceptually novel oscillator based on double CNT@MST hetero-nanotubes, and performed the classical molecular dynamics simulations to understand the effect of both the inter-tube gap width and the chirality of the oscillator inner and outer tubes on the oscillation characteristics of the inner tube. Our simulation results show that a smooth and stable oscillator with a frequency reaching 20 GHz can be obtained based on double-walled CNT@MST hetero-nanotubes for a wide range of gap widths, demonstrating a stronger advantage over oscillators that are built from DWCNTs. We also found that the off-axial rocking motion of the inner tube increases with increasing the gap width, resulting in a more significant energy loss of the inner tube. In addition, we found that the oscillation characteristics of CNT@MST oscillators with different inner and outer tube chirality are much better than those of CNT@MST oscillators containing two tubes with the same chirality.

Acknowledgements

This work was supported by the National Natural Science Foundation of China (Nos. 11162014 and 11372126).

References

[1] Iijima, S. Helical microtubules of graphitic carbon. *Nature* **1991**, *354*, 56–58.

[2] Janas, D.; Koziol, K. K. A review of production methods of carbon nanotube and graphene thin films for electrothermal applications. *Nanoscale* **2014**, *6*, 3037–3045.

[3] Qin, Z.; Zou, J.; Feng, X. Q. Influence of water on the frequency of carbon nanotube oscillators. *J. Comput. Theor. Nanos.* **2008**, *5*, 1403–1407.

[4] Shen, C.; Brozena, A. H.; Wang, Y. H. Double-walled carbon nanotubes: Challenges and opportunities. *Nanoscale* **2011**, *3*, 503–518.

[5] Lee, S. W.; Campbell, E. E. B. Nanoelectromechanical devices with carbon nanotubes. *Curr. Appl. Phys.* **2013**, *13*, 1844–1859.

[6] Rasekh, M.; Khadem, S. E.; Toghraee, A. NEMS thermal switch operating based on thermal expansion of carbon nanotubes. *Phys. E: Low Dimens. Syst. Nanostr.* **2014**, *59*, 210–217.

[7] Remškar, M.; Viršek, M.; Mrzel, A. The MoS_2 nanotube hybrids. *Appl. Phys. Lett.* **2009**, *95*, 133122.

[8] Ferrari, A. C.; Bonaccorso, F.; Fal'Ko, V.; Novoselov, K. S.; Roche, S.; Bøggild, P.; Borini, S.; Koppens, F. H. L.; Palermo, V.; Pugno, N. et al. Science and technology roadmap for graphene, related two-dimensional crystals, and hybrid systems. *Nanoscale* **2015**, *7*, 4598–4810.

[9] Seifert, G.; Terrones, H.; Terrones, M.; Jungnickel, G.; Frauenheim, T. Structure and electronic properties of MoS_2 nanotubes. *Phys. Rev. Lett.* **2000**, *85*, 146–149.

[10] Song, I.; Park, C.; Choi, H. C. Synthesis and properties of molybdenum disulphide: From bulk to atomic layers. *RSC Adv.* **2015**, *5*, 7495–7514.

[11] Zhuiykov, S.; Kats, E. Atomically thin two-dimensional materials for functional electrodes of electrochemical devices. *Ionics* **2013**, *19*, 825–865.

[12] Dallavalle, M.; Sändig, N.; Zerbetto, F. Stability, dynamics, and lubrication of MoS_2 platelets and nanotubes. *Langmuir* **2012**, *28*, 7393–7400.

[13] Mak, K. F.; McGill, K. L.; Park, J.; McEuen, P. L. The valley Hall effect in MoS_2 transistors. *Science* **2014**, *344*, 1489–1492.

[14] Sarkar, D.; Liu, W.; Xie, X. J.; Anselmo, A. C.; Mitragotri, S.; Banerjee, K. MoS_2 field-effect transistor for next-generation label-free biosensors. *ACS Nano* **2014**, *8*, 3992–4003.

[15] Bertolazzi, S.; Krasnozhon, D.; Kis, A. Nonvolatile memory cells based on MoS_2/graphene heterostructures. *ACS Nano* **2013**, *7*, 3246–3252.

[16] Ma, L.; Chen, W. X.; Xu, Z. D.; Xia, J. B.; Li, X. Carbon nanotubes coated with tubular MoS_2 layers prepared by hydrothermal reaction. *Nanotechnology* **2006**, *17*, 571–574.

[17] Song, X. C.; Zheng, Y. F.; Zhao, Y.; Yin, H. Y. Hydrothermal synthesis and characterization of CNT@MoS_2 nanotubes. *Mater. Lett.* **2006**, *60*, 2346–2348.

[18] Zhang, X. F.; Luster, B.; Church, A.; Muratore, C.; Voevodin, A. A.; Kohli, P.; Aouadi, S.; Talapatra, S. Carbon nanotube–MoS_2 composites as solid lubricants. *ACS Appl. Mater. inter.* **2009**, *1*, 735–739.

[19] Wang, J. Z.; Lu, L.; Lotya, M.; Coleman, J. N.; Chou, S. L.; Liu, H. K.; Minett, A. I.; Chen, J. Development of MoS_2–CNT composite thin film from layered MoS_2 for lithium batteries. *Adv. Energy Mater.* **2013**, *3*, 798–805.

[20] Yuan, H. Y.; Li, J. Y.; Yuan, C.; He, Z. Facile synthesis of MoS_2@CNT as an effective catalyst for hydrogen production in microbial electrolysis cells. *ChemElectroChem* **2014**, *1*, 1828–1833.

[21] Maharaj, D.; Bhushan, B. Characterization of nanofriction of MoS_2 and WS_2 nanotubes. *Mater. Lett.* **2015**, *142*, 207–210.

[22] Li, N. N.; Lee, G.; Jeong, Y. H.; Kim, K. S. Tailoring electronic and magnetic properties of MoS_2 nanotubes. *J. Phys. Chem. C* **2015**, *119*, 6405–6413.

[23] Maharaj, D.; Bhushan, B. Nanomechanical behavior of MoS_2 and WS_2 multi-walled nanotubes and carbon nanohorns. *Sci. Rep.* **2015**, *5*, 8539.

[24] Lorenz, T.; Teich, D.; Joswig, J. O.; Seifert, G. Theoretical study of the mechanical behavior of individual TiS_2 and MoS_2 nanotubes. *J. Phys. Chem. C* **2012**, *116*, 11714–11721.

[25] Kis, A.; Mihailovic, D.; Remskar, M.; Mrzel, A.; Jesih, A.; Piwonski, I.; Kulik, A. J.; Benoît, W.; Forró, L. Shear and Young's moduli of MoS_2 nanotube ropes. *Adv. Mater.* **2003**, *15*, 733–736.

[26] Li, W. F.; Zhang, G.; Guo, M.; Zhang, Y. W. Strain-tunable electronic and transport properties of MoS_2 nanotubes. *Nano Res.* **2014**, *7*, 518–524.

[27] Xiao, J.; Long, M. Q.; Li, X. M.; Xu, H.; Huang, H.; Gao, Y. L. Theoretical prediction of electronic structure and carrier mobility in single-walled MoS_2 nanotubes. *Sci. Rep.* **2014**, *4*, 4327.

[28] Enyashin, A. N.; Ivanovskii, A. L. Modeling of the capillary filling of MoS_2 nanotubes with titanium tetrachloride molecules. *Theor. Exp. Chem.* **2010**, *46*, 203–207.

[29] Enyashin, A. N.; Seifert, G. Molecular-dynamics simulations of capillary imbibition of KI melt into MoS_2 nanotubes. *Chem. Phys. Lett.* **2010**, *501*, 98–102.

[30] Bucholz, E. W.; Sinnott, S. B. Mechanical behavior of MoS_2 nanotubes under compression, tension, and torsion from molecular dynamics simulations. *J. Appl. Phys.* **2012**, *112*, 123510.

[31] Brenner, D. W.; Shenderova, O. A.; Harrison, J. A.; Stuart, S. J.; Ni, B.; Sinnott, S. B. A second-generation reactive empirical bond order (REBO) potential energy expression for hydrocarbons. *J. Phys.-Condens. Mat.* **2002**, *14*, 783–802.

[32] Stillinger, F. H.; Weber, T. A. Computer simulation of local order in condensed phases of silicon. *Phys. Rev. B* **1985**, *31*, 5262–5271.

[33] Jiang, J. W. Parametrization of Stillinger-Weber potential based on valence force field model: Application to single-layer MoS_2 and black phosphorus. *Nanotechnology* **2015**, *26*, 315706.

[34] Jiang, J. W.; Park, H. S.; Rabczuk, T. Molecular dynamics simulations of single-layer molybdenum disulphide (MoS_2): Stillinger-Weber parametrization, mechanical properties, and thermal conductivity. *J. Appl. Phys.* **2013**, *114*, 064307.

[35] Jiang, J. W.; Park, H. S.; Rabczuk, T. MoS_2 nanoresonators: Intrinsically better than graphene? *Nanoscale* **2014**, *6*, 3618–3625.

[36] Zou, J.; Ji, B. H.; Feng, X. Q.; Gao, H. J. Molecular-dynamic studies of carbon–water–carbon composite nanotubes. *Small* **2006**, *2*, 1348–1355.

[37] Liu, P.; Zhang, Y. W.; Lu, C. Analysis of the oscillatory behavior of double-walled carbon nanotube-based oscillators. *Carbon* **2006**, *44*, 27–36.

[38] Jiang, J. W.; Park, H. S. Mechanical properties of MoS_2/graphene heterostructures. *Appl. Phys. Lett.* **2014**, *105*, 033108.

[39] Tomar, D. S.; Singla, M.; Gumma, S. Potential parameters for helium adsorption in silicalite. *Micropor. Mesopor. Mat.* **2011**, *142*, 116–121.

[40] Rouha, M.; Moučka, F.; Nezbeda, I. The Effect of cross interactions on mixing properties: Non-Lorentz-Berthelot Lennard-Jones mixtures. *Collect. Czech. Chem. C.* **2008**, *73*, 533–540.

[41] Rouha, M.; Nezbeda, I. Non-Lorentz-Berthelot Lennard-Jones mixtures: A systematic study. *Fluid Phase Equilibr.* **2009**, *277*, 42–48.

[42] Stuart, S. J.; Tutein, A. B.; Harrison, J. A. A reactive potential for hydrocarbons with intermolecular interactions. *J. Chem. Phys.* **2000**, *112*, 6472–6486.

[43] Kang, J. W.; Kim, K. S.; Hwang, H. J.; Kwon, O. K. Molecular dynamics study of effects of intertube gap on frequency-controlled carbon-nanotube oscillators. *Phys. Lett. A.* **2010**, *374*, 3658–3665.

[44] Voter, A. F.; Doll, J. D. Transition state theory description of surface self-diffusion: Comparison with classical trajectory results. *J. Chem. Phys.* **1984**, *80*, 5832–5838.

[45] Doll, J. D.; McDowell, H. K. Theoretical studies of surface diffusion: Self-diffusion in the fcc (111) system. *J. Chem. Phys.* **1982**, *77*, 479–483.

[46] Miwa, R. H.; Scopel, W. L. Lithium incorporation at the MoS_2/graphene interface: An *ab initio* investigation. *J. Phys.-Condens. Matter.* **2013**, *25*, 445301.

[47] Servantie, J.; Gaspard, P. Rotational dynamics and friction in double-walled carbon nanotubes. *Phys. Rev. Lett.* **2006**, *97*, 186106.

[48] Cumings, J.; Zettl, A. Low-friction nanoscale linear bearing realized from multiwall carbon nanotubes. *Science* **2000**, *289*, 602–604.

[49] Zheng, Q. S.; Jiang, Q. Multiwalled carbon nanotubes as gigahertz oscillators. *Phys. Rev. Lett.* **2002**, *88*, 045503.

[50] Zhao, Y.; Ma, C. C.; Chen, G. H.; Jiang, Q. Energy dissipation mechanisms in carbon nanotube oscillators. *Phys. Rev. Lett.* **2003**, *91*, 175504.

[51] Guo, W. L.; Guo, Y. F.; Gao, H. J.; Zheng, Q. S.; Zhong, W. Y. Energy dissipation in gigahertz oscillators from multiwalled carbon nanotubes. *Phys. Rev. Lett.* **2003**, *91*, 125501.

[52] Belikov, A. V.; Lozovik, Y. E.; Nikolaev, A. G.; Popov, A. M. Double-wall nanotubes: Classification and barriers to walls relative rotation, sliding and screwlike motion. *Chem. Phys. Lett.* **2004**, *385*, 72–78.

[53] Rivera, J. L.; McCabe, C.; Cummings, P. T. The oscillatory damped behaviour of incommensurate double-walled carbon nanotubes. *Nanotechnology* **2005**, *16*, 186–198.

[54] Legoas, S. B.; Coluci, V. R.; Braga, S. F.; Coura, P. Z.; Dantas, S. O.; Galvão, D. S. Molecular-dynamics simulations of carbon nanotubes as gigahertz oscillators. *Phys. Rev. Lett.* **2003**, *90*, 055504.